

Ionospheric Scintillation in Brazil: Analysis and Its Impact on GNSS Loss of Lock

João Lucas Eulino Alves Silva¹, Daniele Barroca Marra Alves¹, Gabriel Oliveira Jerez¹, João Francisco Galera Monico¹, Daniel Dionisio de Freitas¹, Raphael Silva Nespolo¹, Tayná Aparecida Ferreira Gouveia¹, João Pedro Voltare Zaupa¹

¹FCT-UNESP, Universidade Estadual Paulista Júlio de Mesquita Filho, 19060-900 Presidente Prudente, Brasil - cei.fct@unesp.br

Keywords: Ionosphere, Scintillation, Loss of Lock, GNSS

Abstract

This study analyses the ionospheric scintillations over the Brazilian territory, focusing on their magnitude, seasonality, and impact on Global Navigation Satellite Systems (GNSS) signal quality, specifically GPS (Global Positioning System), GLONASS (Global'naya Navigatsionnaya Sputnikovaya Sistema / Global Navigation Satellite System) and GALILEO. The main objective is to quantify and evaluate how such phenomena affect positioning integrity by establishing relationships between scintillation intensity, expressed by the S4 index, and signal loss events (Loss of Lock). Additionally, a statistical and temporal analysis of satellite availability per hour for different GNSS constellations is conducted, assessing their variability and reliability. Data are obtained using the ISMR (Ionospheric Scintillation Monitor Receivers) Query Tool platform, which provides information from several GNSS stations over Brazil. The analysis was carried out using SQL queries and MATLAB-developed algorithm. The results contributed to a better subject to signal degradation. A significant correlation was observed between scintillation intensity and periods of high solar activity, particularly in 2014. Furthermore, although most loss of lock events were expected during strong scintillation, approximately 83% occurred during low S4 index intervals (<0.29), suggesting other contributing factor or limitations in S4 data availability during signal interruptions

1. Introduction

In geodesy, the atmosphere is divided into two layers: the neutral atmosphere and the ionosphere. The ionosphere, extending from approximately 50 to 1000 Km in altitude, is influenced by solar radiation, which, along with Earth's magnetic and electric fields, causes irregularities in the electron density (Matsuoka, 2007). Such irregularities can lead to ionospheric scintillation, a phenomenon characterized by rapid fluctuations in the amplitude or phase of a radio wave as it propagates through this environment (Vani, 2013).

This process typically begins after sunset, when ion recombination occurs, leading to a decrease in plasma density in the lower layers of the ionosphere. The most significant effects are observed in the equatorial region, where plasma movement results in areas of high Total Electron Content (TEC), thereby increasing the occurrence of scintillation events.

Since GNSS is widely used in applications that demand high-precision positioning (Langley, Teunissen & Montenbruck, 2017), the presence of ionospheric scintillation has become increasingly problematic. Scintillation events are known to interfere with GNSS signals, degrading their quality and potentially rendering accurate positioning unfeasible (Monico, 2008)

Understanding the spatial distribution of the scintillation phenomenon is of great importance, especially in regions near the Earth's magnetic equator. In these areas, scintillation effects are significantly intensified due to geomagnetic

characteristics. In this sense, the Brazilian region, located within this critical zone is of particular interest.

Several indices can be used to measure the intensity of ionospheric scintillation, such as the S4 index, commonly used for amplitude scintillation. By using specific GNSS receivers, known as Ionospheric Scintillation Monitor Receivers, it is possible to collect GNSS data and compute these indices.

In this context, the present work aims to investigate the phenomenon of ionospheric scintillation in the Brazilian region and assess its impact on GNSS loss of lock, exploring its relationship with amplitude scintillation values, particularly the S4 index, its seasonality, and possible cause-and-effect connections with identified signal loss events.

In order to address these objectives, Section 2 describes the methodology employed in this study, detailing the data acquisition process, the criteria used to identify loss of lock events, and their subsequent classification based on S4 index interval. Section 3 presents and discusses the results obtained from the temporal and spatial analyses of scintillations and signal disruptions across different GNSS constellations and frequencies. Finally, Section 4 provides the main conclusions drawn from the analyses, highlighting the relationship between solar and seasonal variability, GNSS signal reliability, and the importance of multi-constellation and multi-frequency strategies for ensuring robustness in positioning services.

2. Methodology

2.1 Data Source and Stations

The data used in this study is from the database provided by the ISMR (Ionospheric Scintillation Monitor Receivers) Query Tool, available at: <https://ismrquerytool.fct.unesp.br/>, which is continuously being improved and updated. The platform offers scintillation indices and related signal metrics for operational GNSS receivers distributed across the Brazilian territory, Figure 1. The nationwide monitoring infrastructure enables the daily generation and storage of over ten million observational data points.



Figure 1 – Ionospheric Scintillation Monitoring Stations – INCT GNSS NavAer Network. The stations analysed in this study are highlighted by colour: FRTZ (red), PALM (orange), PRU2 (green), and POAL (yellow).

This tool is an integral part of the INCT (Instituto Nacional de Ciências e Tecnologia - National Institute of Science and Technology) GNSS-NavAer project. In this study, data acquired through the web-based software is subjected to a filtering process directly on the platform using SQL (Structured Query Language) queries. During this process, only records with an elevation angle equal to or greater than 30° are considered, aiming to mitigate multipath effects.

To analyse the data acquired from the database, it is considered the following variables: *time_utc* (Coordinated Universal Time), *S4* (scintillation intensity index), *SVID* (Space Vehicle Identification), *elevation* (angle between the satellite and the horizon), *locktime_l1* (lock time on L1), *locktime_l2* (lock time on L2), and *locktime_l5* (lock time on L5).

2.2 Identification of Loss of Lock Events

To identify loss of lock (LoL) events, both *locktime* data and *S4* temporal data are evaluated for the same *SVID*. The *locktime* variable indicates the number of seconds during which a GNSS receiver has continuously tracked a satellite signal. As long as the satellite remains visible, the *locktime*

counter increases monotonically. However, when the satellite is no longer visible, either because it sets below the elevation mask or due to a Loss of Lock (LoL), the behavior differs.

In the case of a LoL, the *locktime* does not reset, instead, it keeps incrementing internally but no measurements are recorded during the outage, which produces a visible gap in the time series as illustrated in Figure 2.

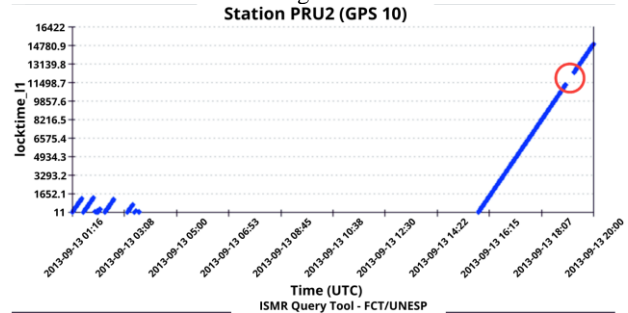


Figure 2 – Expected behavior of the *locktime* variable during LoL indicated in red

For instance, if the variable *locktime* acquired by a GNSS receiver reaches 1200 s prior to a Loss of Lock event, and the subsequent available record indicates a value of 1250 s, the interval between 1200 and 1250 s can be interpreted as the duration of the signal interruption, thereby characterizing a Loss of Lock. This property makes *locktime* a reliable parameter to identify LoL events without confusing them with normal satellite setting, where the counter restarts from zero.

In this study, *locktime* values for the L1, L2C, and L5 bands were used as primary indicators of LoL events. A gap longer than 60 seconds between consecutive *locktime* records was considered a potential loss of lock, since the data are logged at on-minute intervals. This approach allows the algorithm to approximate the scintillation conditions at the time of each LoL by associating the most recent *S4* index measurement with the corresponding event. In a second case, discontinuities longer than one minute in the *time_utc* variable for scintillation data were examined.

In each case, losses of lock events are independently flagged in the scintillation dataset according to the respective methodology, allowing for separate identification and subsequent comparison between the two approaches.

Additionally, a time limit is established for loss of lock events identified through *time_utc*, considering both satellite orbits (and the resulting loss of visibility) and the magnitude of the observed results, which will be further discussed.

Due to its continuous nature, when a signal interruption occurs due to a loss of lock, the *locktime* variable continues incrementing, thereby creating a gap during the period the signal is unavailable. This behavior enables the identification of the LoL event. Upon detecting a LoL, the algorithm records the last available *S4* index value and assigns it to the loss of lock event, allowing for an approximation of ionospheric scintillation behavior at the moment.

2.3 Scintillation Classification and Station Selection

Finally, S4 values can be classified according to the Srinivasu et al. (2018), which defines three scintillation intensity ranges: weak ($S4 < 0.29$), moderate ($0.30 < S4 < 0.45$), and strong ($S4 > 0.45$), for the period analysed between July 2014 and August 2016.

The stations selected for the study are PALM (Palmas, TO), POAL (Porto Alegre, RS), PRU2 (Presidente Prudente, SP), and FRTZ (Fortaleza, BA). These stations are geographically distributed across distinct regions of Brazil, with FRTZ and PALM located closer to the magnetic equator, while PRU2 and POAL are situated further south.

This spatial distribution is relevant due to the fountain effect, which refers to the influence of Earth’s magnetic field on electron motion. This effect causes electrons to move along the horizontal magnetic field lines away from the equator, resulting in regions of high electron concentration (Camargo, 1999). The areas of greatest Total Electron Content (TEC) are typically found between $\pm (15^\circ - 20^\circ)$ from the magnetic equator (Seeber, 2003).

2.4 Solar Cycle and Seasonal Variability of Scintillation

The period selected for analysis of the present study was determined through visual inspection, aimed at identifying patterns, scintillation intensities, and as well, possible loss of lock events. For comparisons of data between stations in the ISMR network, periods with simultaneous data availability across the selected stations were chosen. An initial step involved observing the solar cycle using the F10.7 index, as shown in Figure 3, in order to correlate solar activity with scintillation intensity.

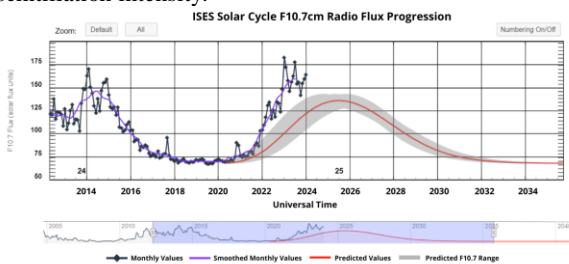


Figure 3 – Solar cycle progression based on F10.7cm Radio Flux: forecast values in red, prediction range in gray, smoothed monthly values in blue, and monthly values in black

It can be observed that years 2013 and 2014 present higher values of the F10.7 index, indicating an intensification of solar activity. In contrast, an analysis of the year 2019 and 2020 reveals significantly lower values for this index, characterizing this period as one of minimal solar activity.

To compare the influence of the solar cycle on scintillation phenomena, calendars with average S4 index values are obtained for both 2014 and 2014, years of high solar activity, and for 2019 and 2020, which represents a period of low solar activity. Additionally, the years 2022 and 2023 were included in the comparison, as they marked a return too elevated values in the solar cycle. All data used in this comparison refer to the PRU2 station, located in Presidente Prudente, where UNESP (Universidade Estadual Paulista) is situated. These results are shown in Figure 4, Figure 5, and Figure 6 respectively.

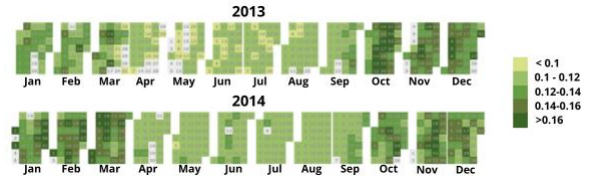


Figure 4 – Daily mean of S4 index values on L1 from GPS satellites for station PRU2 in 2013 and 2014

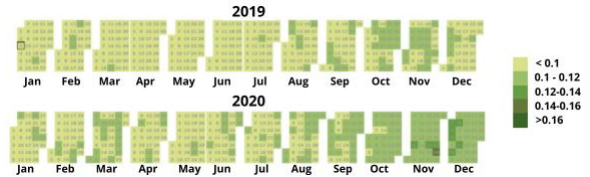


Figure 5 – Daily mean of S4 index values on L1 from GPS satellites for station PRU2 in 2019 and 2020

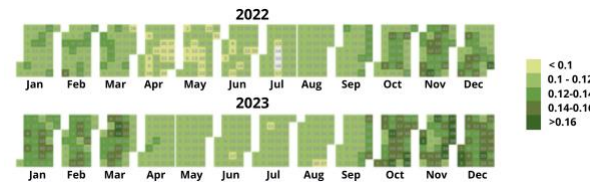


Figure 6 – Daily mean of S4 index values on L1 from GPS satellites for station PRU2 in 2022 and 2023

A significant correlation can be observed between scintillation events and periods of higher and lower solar activity. During the years of 2013 and 2014, which correspond to a phase of increased solar activity, higher daily average scintillation intensities are recorded at the PRU2 station. In contrast, years of lower solar activity, such as 2019 and 2020, the corresponding daily averages of scintillation observed at the same PRU2 station show reduced intensity.

In the more recent period of 2022 and 2023, as F10.7 solar activity values begin to rise again, S4 index values also return to elevated levels. This observation suggests that scintillation phenomena do not occur randomly but are closely tied to the natural rhythms of the solar cycle, reflecting significant variations in accordance with its active and quiet phases.

It is also worth noting that ionospheric scintillation is particularly pronounced during the equinox periods and the summer solstice, highlighting the seasonal nature of these events. This pattern indicates the strong influence of seasonal variations on the occurrence and intensity of scintillations.

3. Results and analysis

The year 2014, characterized as a peak period of solar activity stood out for exhibiting high average S4 values. Figure 7 presents the daily S4 values on L1 for GPS satellites from station PRU2 in 2014.

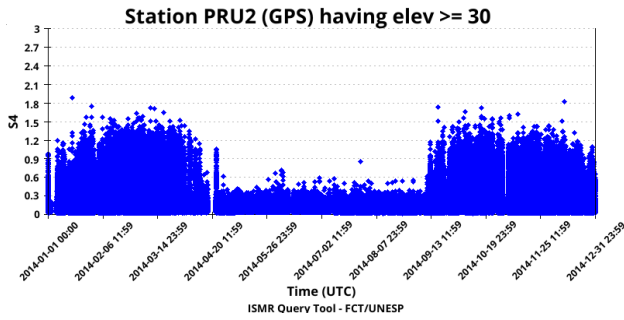


Figure 7 – Daily S4 values on L1 from GPS satellites for station PRU2 in 2014

In 2014, S4 values remained high, especially during the equinoxes and the summer solstice. These values reinforce the dynamics of 2014 in terms of ionospheric disturbances, showing how intense solar activity and seasonality can directly influence the variability and intensity of scintillation, and, consequently, of such indices.

Initially, to improve the understanding and interpretation of loss of lock phenomena, the focus is placed on identifying and assessing loss of lock occurrences. Initially, to interpret the results, loss of lock events is identified based on time gaps greater than one minute in the time_utc and S4 datasets, with a 30° elevation angle threshold applied to reduce multipath effects, as explained in methodology section.

To refine the analysis and avoid spurious results, lower and upper duration thresholds were established, ranging from 1 to 240 minutes. This filtering process led to the output presented in Figure 8.

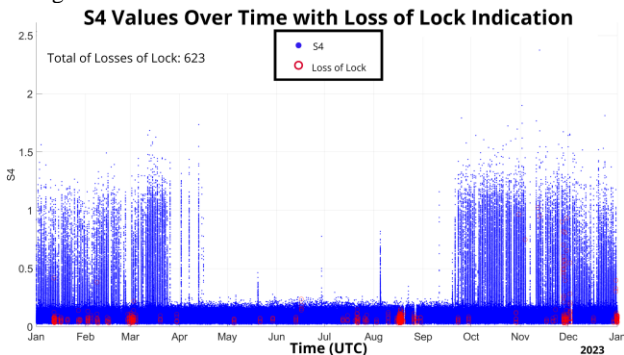


Figure 8 – S4 index over time from GPS satellite data for station PRU2 in 2023, with loss of lock events between 1 and 240 minutes marked in red

It is possible to observe in Figure 8 that losses of lock events occurred under both low and high scintillation conditions. Furthermore, a remarkably large number of LoL events was recorded in August, a period during which fewer occurrences would typically be expected. Therefore, a specific analysis was carried out for this interval, as shown in Figure 9.

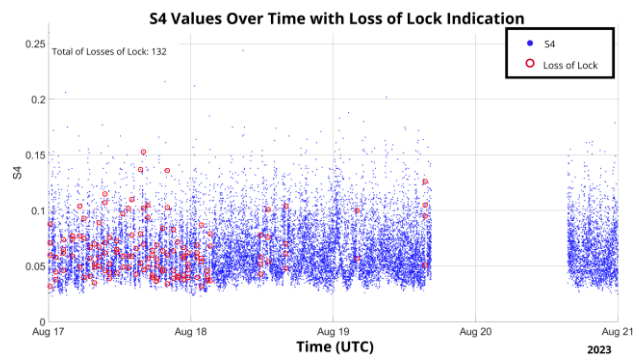


Figure 9 – S4 index over time with losses of lock from GPS satellite data for station PRU2, August 17-20, 2023

The distribution of losses of lock shown in Figure 9, characterized by a high incidence over a short time span and deviating from the expected seasonal pattern, prompted a more in-depth analysis. Therefore, the behavior of the locktime_11 variable was examined for selected satellites that experienced losses of lock during this period, as illustrated in Figure 10, in order to gain a better understanding of these occurrences.

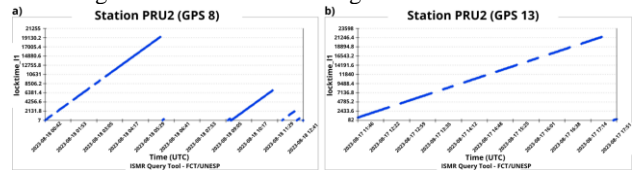


Figure 10 – Locktime_11 values over time for GPS 8 on the 18th (a) and for GPS 13 on the 17th (b)

This detailed analysis shown at Figure 10 revealed that, even outside the expected seasonal pattern, the loss of lock events concentrated in August, Figure 9, exhibited the expected behavior of LoL events, characterized by rapid variations. This behavior is evidenced by the significant segmentation in the locktime_11 index, indicating that signal reacquisition occurred promptly, with interruptions lasting only a few minutes in the continuous graph.

The study is also extended to include the L2C and L5 frequencies, as shown in Figure 11 and Figure 12 respectively. From this point onward, the identification of losses of lock relied exclusively on the methodology based on the locktime data.

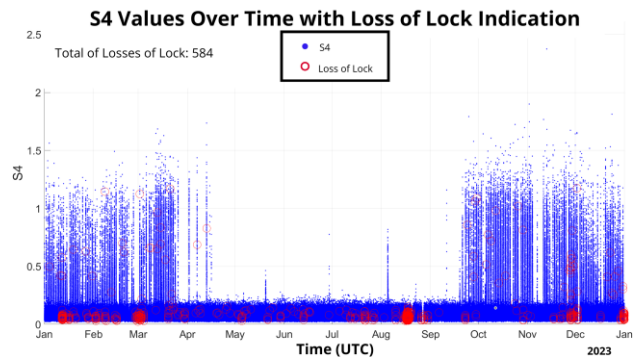


Figure 11 – Loss of lock signaling for the PRU2 station in 2023 on the L2C band

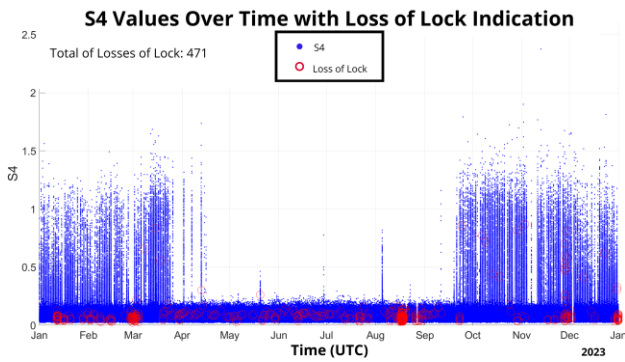


Figure 12 – Loss of lock signaling for the PRU2 station in 2023 on the L5 band

The reliability of the current GPS system is supported by the comparison of the results regarding both the seasonality and the number of losses of lock events. The small variation, only 279 occurrences between the maximum and minimum, observed in the values highlights the consistent behavior of these events across different frequency bands, whether L1 (750), L2 (584), or even L5 (471).

The spatial distribution of the phenomenon is also investigated assessing how loss of lock occurrences manifests in different regions of Brazil, with the aim of identifying areas with higher or lower incidence across various latitudes. For this purpose, March 2014 is selected, this period was chosen to observe loss of lock behavior taking into account the high S4 index values and the data availability for each station.

A comparison of loss of lock events among the selected stations was carried out by analysing gaps in the locktime_l1 variable, taking into account the expected influence of these ionospheric characteristics across latitudes

The results show a relatively consistent distribution of LoL events across the stations, with 85 occurrences observed at FRTZ, 45 at PALM, 41 at POAL, and 22 at PRU2. Although it was initially expected that LoL events would be more concentrated in periods or locations associated with higher S4 index values a higher number of events is observed at FRTZ. However, the overall analysis indicated that both number of losses of lock and the corresponding scintillation levels did not vary significantly among the stations, despite their different geographic positions.

Table 1 presents the number of losses of lock events within specific S4 value intervals.

STATION	0.01 – 0.29	0.30 – 0.45	>0.45
POAL	26	1	14
FRTZ	82	2	1
PALM	42	0	3
PRU2	10	1	11

Table 1 – Number of losses of lock in S4-defined intervals for the stations POAL, FRTZ, PALM, and PRU2 in March 2014

When examining the S4 index value intervals, a clear predominance of low values, ranging from 0.01 to 0.29 is evident, accounting for approximately 83% of the total loss of lock events. The prevalence of these values reinforces the behavior observed in previous figures. This behavior contradicted initial expectations, as it is anticipated that loss of

lock would be primarily associated with higher S4 values, particularly those exceeding 0.45. This result may be attributed to the unavailability of observables at the exact moment of the LoL, making it possible only to infer ionospheric behavior based on data preceding the event.

After that, the study also assessed data from other GNSS, with particular attention to GLONASS, the Russian high-orbit satellite navigation system. A graphical analysis was conducted, as presented in Figure 13, to support this assessment. For this analysis, data from the L2 frequency band were used through the locktime_l2 variable.

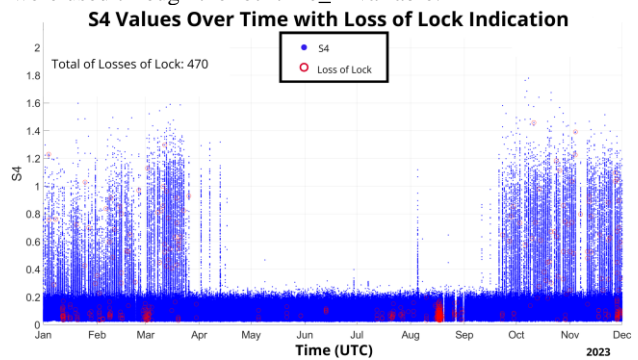


Figure 13 – S4 index over time from GLONASS satellite data for station PRU2 in 2023, with loss of lock events for the L2C band marked in red

The values obtained for GLONASS reinforce the results from GPS, demonstrating consistency in the loss of lock products across these systems and, to some extent, confirming system reliability. A noteworthy outcome is the lower number of losses of lock events recorded for GLONASS, 470 compared to 584 for GPS, representing a 19.52% reduction.

Finally, a comparative analysis is performed for the GPS, GLONASS and Galileo constellations using the same locktime_l2 metric for GPS and GLONASS and the equivalent E5a band for Galileo. March 2023 is selected as the study period, specifically due to the presence of elevated scintillation levels observed during this month for the Brazilian region.

The three systems displayed broadly similar numbers of LoL events, 65 for GPS, 57 for GLONASS, and 55 for Galileo, indicating comparable operation performance. Nevertheless, GLONASS is associated with noticeably higher S4 values during those LoL events, suggesting that its signal interruptions are more strongly linked to intense scintillation than those of GPS or Galileo.

A comparison regarding satellite availability for the different systems in the years 2014 (Figure 14) and 2023 (Figure 15), covering the period from March 17 to 20. The analysis is based on an hourly evaluation, identifying the highest number of satellites available at each time, for all frequency bands recorded in the ISMR Query Tool database.

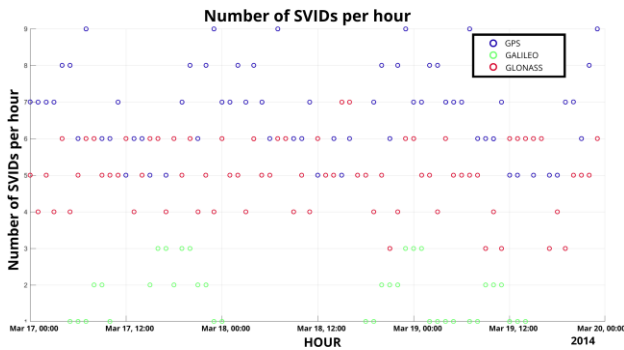


Figure 14 – Hourly satellite availability of the GPS, GLONASS, and Galileo systems from March 17 to 20, 2014

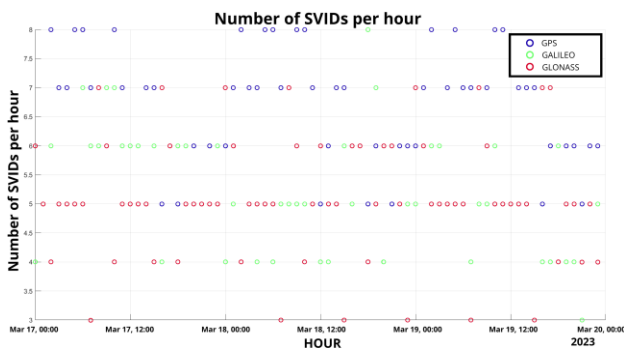


Figure 15 – Hourly satellite availability of the GPS, GLONASS, and Galileo systems from March 17 to 20, 2023

It is found that the GPS system had the highest number of active satellites throughout the day, maintaining an average of 6 to 7 satellites available per hour in 2014 and 2023. Followed by the GLONASS system, which exhibited slightly lower availability, with an average of approximately 5 satellites available per hour in both years. A noteworthy point is the progress of the Galileo system, which in 2014 shows a very limited availability, with an average of fewer than 2 satellites. However, in the 2023 evaluation, it reaches values comparable to those of the GPS system at certain times, with an average close to that of the GLONASS system, around 5 satellites available per hour. This demonstrates the advancement of the Galileo system and reinforces the reliability of using GNSS.

4. Conclusion

This research provides a closer view of the temporal variation of ionospheric scintillation, the evidence suggests that scintillation events are not random; rather, they align with the natural rhythms of solar activity, displaying marked differences between solar-maximum and solar-minimum periods. Seasonality is another key factor: scintillation levels rise noticeably around the equinoxes and the summer solstice, confirming that these specific times of year are particularly critical for the GNSS operations.

Considering loss of lock events, a significant share of the interruptions occurred in conjunction with low-intensity scintillation ($S4 < 0.29$). This outcome may stem from the very nature of a loss of lock: at the moment the receiver loses the signal, $S4$ are often unavailable, leaving only previous measurements to infer ionospheric conditions.

Other factors may also contribute to LoL, including receiver hardware limitations, temporary failures in signal tracking loops, radio-frequency interference, and thermal noise. These aspects highlight the importance of considering complementary indices and external validation with independent data sources in future research, in order to obtain a more comprehensive understanding of the mechanisms underlying signal disruptions.

Comparative analyses across the GPS L1, L2, and L5 bands confirms the reliability of the current system. The minor variability in scintillation values, combined with similar seasonal pattern and LoL statistics across all three bands, points to consistent behavior regardless of frequency. Extending the comparison to different GNSS constellations, GPS, GLONASS, and Galileo, revealed broadly similar trends. Although small differences can be observed in LoL counts and $S4$ values, the overall patterns remain coherent. It is also worth mentioning results underscore the value of multi-constellation solutions for enhancing robustness and reliability in GNSS applications.

The findings highlight the importance of understanding ionospheric dynamics, adopting multi-frequency and multi-constellation strategies, and refining detection methodologies to mitigate scintillation-related signal degradation and ensure dependable positioning services

5. Acknowledgements

To INCT GNSS-NavAer, funded by CNPq (process 465648/2014-2), FAPESP (process 2017/50115-0) and CAPES (process no. 88887.137186/2017-00). FAPESP (process 2021/05285-0)

6. References

Camargo, P. O. Modelo Regional da Ionosfera para uso em Posicionamento com Receptores de uma Frequência. Tese (Doutorado em Ciências Geodésicas) Universidade Federal do Paraná, Curitiba, 1999.

Langley, R.B.; Teunissen, P. J. G.; Montenbruck, O. Introduction to GNSS. In: Langley, R.B; Teunissen, P. J. G.; Montenbruck, O. (eds) Springer Handbook of Global Navigation Satellite Systems. Springer, Berlin, 2017.

Matsuoka, Marcelo Tomio. Influência de diferentes condições da ionosfera no posicionamento por ponto com gps: Avaliação na região brasileira. 2007, Tese de doutorado (Programa de Pós-Graduação em Ciências Cartográficas) – UNESP, São Paulo.

Monico, J.F.G. Posicionamento pelo GNSS: descrição fundamentos e aplicações. São Paulo: Ed. da UNESP, 2008. 476p.

Seeber, G. Satellite geodesy: foundations, methods, and applications. 2nd. ed. Berlin, New York: Walter de Gruyter, 2003. 589p

Srinivasu, V.K.D., Dashora, N., Prasad, D.S.V.V.D. et al. On the occurrence and strength of multi-frequency multi-GNSS

Ionospheric Scintillations in Indian sector during decling phase of solar cycle 24 *Advances in Space Research* 61, 7 (2018)

Srinivasu, V.K.D., Dashora, N., Prasad, D.S.V.V.D. et al. Loss of lock on GNSS signals and its association with ionospheric irregularities observed over Indian low latitudes. *GPS Solut* 26, 34 (2022)

Vani, B.C.; Shimabukuro, M.H.; Monico, J.F.G. Cintilação Ionosférica no Brasil: Aspectos gerais obtidos no monitoramento utilizando a rede Cigala/Calibra VIII Colóquio Brasileiro de Ciências Geodésicas 2013.